

Effects of Vegetation Canopy Density and Bank Angle on Near-Bank Patterns of Turbulence and Reynolds Stresses

Nicole M. Czarnomski¹; Desireé D. Tullós²; Robert E. Thomas³; and Andrew Simon⁴

Abstract: Vegetation growing on the surface of a streambank has been shown to alter the shear stresses applied to the boundary, but basic questions remain regarding the influence of vegetation and streambank configurations on near-bank hydraulics. In the present study, Froude-scaled flume experiments were used to investigate how changes in vegetation density (ratio of frontal area to channel area, including both stems and leaves) and bank surface angle influence near-bank turbulence intensities ($RMS_{u,v,w}$) and Reynolds stresses (τ_{uv} and τ_{uw}) estimated using velocities obtained with an acoustic Doppler velocimeter positioned beneath the canopy. Results illustrate how, with increasing vegetation density, turbulence intensities and Reynolds stresses decreased along the sloped bank surface but increased at the base of the slope and within the main channel. The steeper bank angle resulted in greater vertical stresses on the bank surface than the shallower angle, but lateral momentum exchange was larger than vertical exchange along the base of the slope, regardless of bank angle. Leaves were an important influence on near-bank turbulence intensities and Reynolds stresses, whereas the influence of bank slope was small relative to the influence of vegetation density. DOI: [10.1061/\(ASCE\)HY.1943-7900.0000628](https://doi.org/10.1061/(ASCE)HY.1943-7900.0000628). © 2012 American Society of Civil Engineers.

CE Database subject headings: Riparian land; Vegetation; Turbulence; Reynolds stress; Hydraulics.

Author keywords: Riparian vegetation; Stream bank; Turbulence intensity; Reynolds stress; Vegetation density.

Introduction

Vegetation on the base of streambanks may deflect flow and reduce near-bank velocities and shear stresses but may also induce turbulence, elevate shear stresses, and promote localized scour along the base of the bank surface (Wilkerson 2007; Yang et al. 2007; Gorrick 2009; Hopkinson and Wynn 2009). Vegetation also generates turbulence in the vertical plane at the interface between the canopy and the free-stream (Yang et al. 2007; White and Nepf 2008; Hopkinson and Wynn 2009; Zong and Nepf 2010). Shear layers form at interfaces between vegetated patches and the free-stream, spawning coherent vortices and eddies (Nepf 1999; White and Nepf 2008; Zong and Nepf 2010). Although it has been found in some cases (e.g., Wilkerson 2007; Hopkinson and Wynn 2009) that plant-flow interactions are similar on banks and floodplains and that turbulence levels on inclined nonvegetated and sparsely-vegetated streambanks are sometimes similar (Hopkinson and Wynn 2009), other studies (Nepf 1999; McBride et al. 2007) document elevated turbulence levels within sparsely-treed floodplains relative to the nonvegetated case. This apparent dichotomy suggests

that site-specific conditions, such as the angle of the bank face and/or bank toe, may influence the relationship between vegetation and channel hydraulics (McBride et al. 2007; Wilkerson 2007). Therefore, the objective of the present study is to use a Froude-scaled flume experiment to characterize the interacting influences of bank angle and vegetation density, defined as the ratio of plant frontal area (the area of submerged leaves and stems in a vertical plane perpendicular to the channel centerline) to flow area, on near-bank patterns of shear stress and turbulence.

Methods

Experiments were conducted in a 6.0 m × 0.6 m × 0.6 m recirculating flume set at a fixed slope of 0.01 mm⁻¹. At the inlet, a rock-filled baffle box and 0.30-m long, 0.02-m diameter tubes (flow straighteners) were used to dampen turbulence and provide parallel streamlines. To simulate a sloping bank surface along one side of the flume, a 4.88-m long insert, inclined at either 15 or 30° from the horizontal, was installed immediately downstream of the flow straighteners. Stands of artificial vegetation of two different stem densities (defined as the number of stems per square meter of bank surface) and two different leaf scenarios [leaved (e.g., LD_{lo} , LD_{hi}) and leafless; the prefix L is used throughout the text to denote leaved cases] were installed in a staggered pattern on the bank surface (Fig. 1). Stems for the artificial plants were constructed by using acrylic rods; ten 28-gauge wire branches with 25 × 35 mm flexible leaves made of contact paper were affixed to the rods in a pattern similar to Wilson et al. (2006a) and commencing 60 mm above the base of the stem. Other than the vegetative elements, the boundaries of the flume were smooth; the flume walls were constructed of lacquered marine plywood. Flow depth was controlled by a weir at the outlet, creating a gradually-varied, highly-subcritical ($15644 \leq Re \leq 16095$)

¹Watershed Sciences Dept., Utah State Univ., 5210 Old Main Hill, Logan, UT 84322. E-mail: nicole.czarnomski@usu.edu

²Dept. of Biological and Ecological Engineering, Oregon State Univ., Corvallis, OR (corresponding author). E-mail: desiree.tullos@oregonstate.edu

³Dept. of Geography, Univ. of Hull, Cottingham Road, Hull, HU6 7RX, UK. E-mail: r.e.thomas02@members.leeds.ac.uk

⁴Cardno ENTRIX, 1223 Jackson Ave. East, Suite 301, Oxford, MS 38655. E-mail: andrew.simon@cardno.com

Note. This manuscript was submitted on February 19, 2011; approved on May 11, 2012; published online on May 14, 2012. Discussion period open until April 1, 2013; separate discussions must be submitted for individual papers. This technical note is part of the *Journal of Hydraulic Engineering*, Vol. 138, No. 11, November 1, 2012. © ASCE, ISSN 0733-9429/2012/11-974-978/\$25.00.

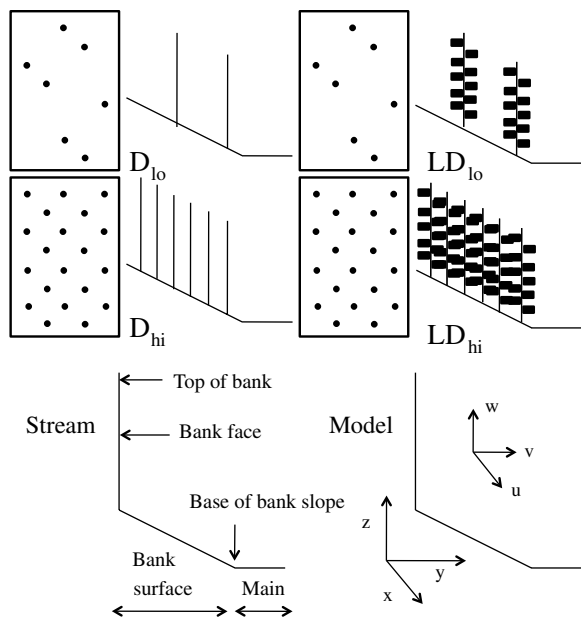


Fig. 1. Experimental design and flume cross-sectional design; D_{lo} is low density, no leaves; D_{hi} is high density, no leaves; LD_{lo} is low density, with leaves; and LD_{hi} is high density, with leaves

Table 1. Flume and Prototype Scaling Parameters

	Scenario	Scaling relation	Model channel	Prototype channel
Geometry				
Bank slope length (m)	15°	λ^{-1}	0.41	2.0
	30°	λ^{-1}	0.46	2.0
Vertical bank face height (m)	15°	λ^{-1}	0.49	2.77
	30°	λ^{-1}	0.37	2.77
Hydraulics				
Main channel flow depth (m)	15°	λ^{-1}	0.38	1.85
	30°	λ^{-1}	0.42	1.85
Cross-sectional mean velocity ^a (ms^{-1})	15°	$\lambda^{1/2}$	0.19	0.40
	30°	$\lambda^{1/2}$	0.21	0.47
Cross-sectional mean Fr (-)	15°	λ^0	0.13–0.16	0.13–0.16
	30°	λ^0	0.15–0.20	0.15–0.20
Vegetation				
Stem density (stems m^{-2})	15°	λ^{-2}	202	10
	30°	λ^{-2}	615	30
Flexural rigidity (Nm^2)	15°	λ^{-5}	0.0435	120.4
	30°	λ^{-5}	0.0435	67.8
Vegetation density (15°; 30° bank surface)	D_{lo}	λ^0	0.027; 0.029	0.027; 0.029
	D_{hi}	λ^0	0.085; 0.103	0.085; 0.103
	LD_{lo}	λ^0	0.155; 0.192	0.155; 0.192
	LD_{hi}	λ^0	0.468; 0.586	0.468; 0.586

Note: Hydraulic parameters are presented as means for all scenarios. The scaling factor, λ , is 4.88 for the 15° bank surface and 4.35 for the 30° bank surface. Froude scaling relations are given by Julien (2002) and Wilson et al. (2003).

^aVelocity in the prototype channel was estimated based on the length scale factor and channel dimensions.

Table 2. Summary Statistics of 64 Evaluations of Bank Slope Length and Bank Slope Angle Estimated from Surveys of Cross-sections 5 and 6 at the Goodwin Creek Bendway, MS

Statistic	Bank slope length (m)	Bank slope angle (°)
Minimum	1.00	8.8
10th percentile	1.71	15.7
16th percentile	1.98	17.3
Median	3.29	22.8
84th percentile	4.63	28.0
90th percentile	4.89	29.4
Maximum	5.61	39.8

Note: These were established at this site in February 1996 and resurveyed at regular intervals until May 2003. The bend apex was initially at cross-section 4 and gradually migrated downstream to between cross-sections 7 and 8.

flow field. Water depths were always less than the height of the plants, and hence, the plants were emergent.

Flume geometry was Froude-scaled from the Goodwin Creek bendway site in North Mississippi (Langendoen and Simon 2008; Simon et al. 2000; Simon and Collison 2002; Wood et al. 2001) to establish both geometric and kinematic similitude (Table 1). Bank slope lengths and angles were computed for repeat surveys at eleven cross-sections at Goodwin Creek, and two (cross-sections 5 and 6; Table 2) were selected for representation in the flume. The 15 and 30° bank angles in our physical model approximate the 10th and 90th percentiles observed in the prototype, respectively. Owing to limitations imposed by the dimensions of the flume, the selected length scales were computed by using the ratios between the model slope lengths (0.41 and 0.46 m, respectively) and the 16th percentile slope length (~2.0 m), rather than the median slope length (3.3 m) of the prototype bank. This scaling approach yielded mean Froude scaling factors of 4.88 and 4.35 for the 15 and 30° bank surface, respectively.

Features (i.e., stem diameter, stem density, frontal area, and flexural rigidity) of the artificial vegetation were also scaled (Table 1). Vegetation models were based on willow and cottonwood yearlings up to 2-m tall and 20-mm diameter, which are commonly found on periodically inundated bank surfaces in densities of ~10 to 30 stems m^{-2} (Wilson et al. 2006b). Thus, applying Froude scaling, artificial plants were constructed using 450-mm long, 4.54-mm diameter acrylic rods and arranged with stem densities of 202 and 615 stems m^{-2} , respectively, in a 3-m long array, beginning immediately downstream of the flow straighteners. The flexural rigidity (J) of stems was also Froude-scaled (Table 1) based on field data collected during the present study (see Czarnomski 2010 for further details) and values reported by others (Niklas 1992; Freeman et al. 2000; Wilson et al. 2003). Reynolds number similarity was necessarily relaxed (Yalin 1971).

Near-Bed Velocity Measurements

Near-bed velocities were measured at seven cross-sections spaced 0.055 m apart at approximately 5 mm above the bed. To limit the influence of conditions imposed at the inlet and outlet, cross-sections were located 1.84–2.23 m downstream from the flow straighteners. Velocities were measured at 25 Hz for 300 s with a downward-looking 10 MHz Nortek acoustic Doppler velocimeter (ADV) that was aligned with the z -axis (see Fig. 1 for a definition of the Cartesian coordinate system employed). Sampling frequency was selected assuming a Strouhal number of 0.21 (e.g., Schlichting 1968), estimating the likely eddy shedding frequency caused

by model stems (9.1–12.3 Hz) and then considering the Nyquist sampling theorem. Sampling duration was selected after analysis of the cumulative velocity variance associated with different sampling windows (e.g., Sukhodolov and Rhoads 2001). The sampling volume of the ADV had a diameter of 6 mm and a volume of 254 mm³, thus capturing turbulent eddies that were approximately as small as the stem diameter. Boundary measurements were made at fixed $x - y$ coordinates for each of the seven cross-sections and were generally located 0.01–0.03 m away from the nearest stem. However, if a velocity sampling location fell within 0.01 m of a stem, that stem was temporarily removed to permit data acquisition. ADV data with correlation coefficients <0.6 and signal-to-noise ratios <0.15 dB were removed and the remaining data were despiked using the phase-space threshold algorithm (Goring and Nikora 2002) within WinADV version 2.027 (Wahl 2009).

Analysis of Velocity Measurements

Using near-bed velocities measured at the cross-section 2.0 m from the beginning of the vegetation, the root mean square (RMS) difference between the instantaneous velocities (u , v , and w) in the streamwise (x), lateral (y), and vertical (z) directions and their respective time-averages (\bar{u} , \bar{v} and \bar{w}) were computed to represent turbulence intensity (Hinze 1975) and to provide an indication of where shear stresses were highest (Biron et al. 2004; Hopkinson and Wynne 2009). Computed values of RMS were normalized by the cross-sectional mean velocity (U) to facilitate comparison of the three components and to illustrate the magnitude of turbulent fluctuations relative to the mean flow.

Local estimates of lateral and vertical Reynolds stresses (τ_{uv} and τ_{uw} , respectively) were used as proxies for applied shear stress (e.g., Biron et al. 2004) and to quantify the magnitude and direction of turbulent fluctuations that represent momentum exchange across a given plane (Robert 2003). τ_{uv} and τ_{uw} were estimated for all sampling points by using $\tau_{uv} = -\rho \overline{u'v'}$ and $\tau_{uw} = -\rho \overline{u'w'}$, respectively, where primes denote fluctuations about the time averaged velocities.

Results

Relative Turbulence Intensity

The presence of vegetation on the bank surface generally increased relative turbulence intensity (RMS/ U) at the base of the bank slope and immediately adjacent to the bank (Fig. 2). For example, at the base of the bank slope, RMS/ U increased by 120–650% over the nonvegetated scenario for LD_{lo} , LD_{hi} and D_{hi} . At this location, values of RMS/ U were also much higher for leaved than for leafless vegetation. For example, relative to the nonvegetated case, at the base of the 15° slope, RMS_u/U , RMS_v/U , and RMS_w/U increased by 60–150% during leafless vegetated runs but by 220–320% during leaved runs (Fig. 2). A similar result was true for the 30° bank; at the base of the bank slope, RMS/ U increased by 140–220% during leafless runs and by 350–650% during leaved runs (Fig. 2).

Streamwise RMS_u/U ranged from 85–160% of the lateral RMS_v/U and from 210–490% of the vertical RMS_w/U . The differences in intensity were similar for the 15 and 30° bank slopes, although the peak magnitude of RMS_u/U on the 30° bank was up to 30% larger than RMS_u/U on the 15° bank, and RMS_v/U was 100% larger on the 30° bank than RMS_v/U on the 15° bank.

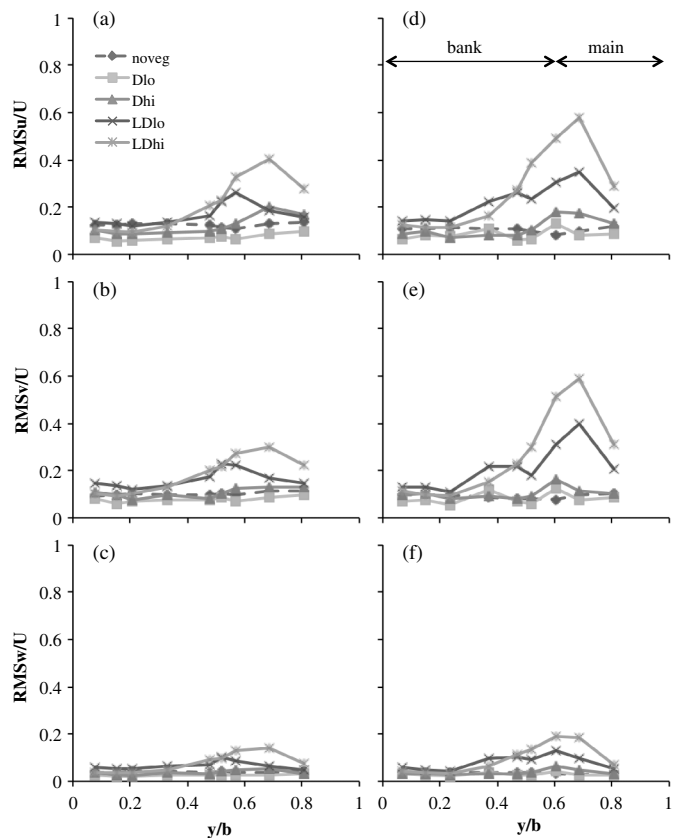


Fig. 2. Cross-stream variations of near-boundary RMS/ U in the u (longitudinal), v (transverse), and w (vertical) directions for the 15° (a, b, c) and 30° (d, e, f) bank surfaces; velocities were measured 2.0 m downstream from the beginning of the vegetation; cross-stream position (y) was normalized by channel width (b); and D_{lo} , D_{hi} , LD_{lo} , and LD_{hi} are defined in Fig. 1

Reynolds Stresses

Spatial patterns of near-bed values of τ_{uw} and τ_{uv} were similar to patterns of RMS/ U , where values were generally positive and increases in stress were observed with increasing plant density. Without vegetation, τ_{uw} values were generally positive (0–0.05 Pa) and were mostly distributed uniformly throughout the cross-section (Fig. 3). Once vegetation was introduced, values of τ_{uw} were positive within the main channel, with a local maximum near the center of the main channel, and negative on the bank surface, with a local minimum near the base of the slope (Fig. 3). The τ_{uw} was up to an order of magnitude lower for the 15° bank than the 30° bank, and the magnitude of τ_{uw} at the stationary points (e.g., maxima, minima) increased with increasing vegetation density (Fig. 3). Similar patterns were observed for τ_{uv} , where increasing vegetation led to higher values of τ_{uv} , indicating increases in lateral momentum exchange across the base of the slope. However, the magnitude of τ_{uv} across the slope base was similar along the 15 and 30° banks (Fig. 4).

The dominant orientation of stresses and momentum exchanges was more variable on the 15° bank than the 30° bank (Figs. 3 and 4). For the 30° bank, lateral momentum exchange was the primary stress found throughout the channel when vegetation was not present. With high density vegetation along the 30° bank, the primary stress on the bank surface was τ_{uw} , whereas τ_{uv} was higher along the base of the slope and in the main channel. For the 15° bank, τ_{uv} was dominant at the base of the slope when no vegetation

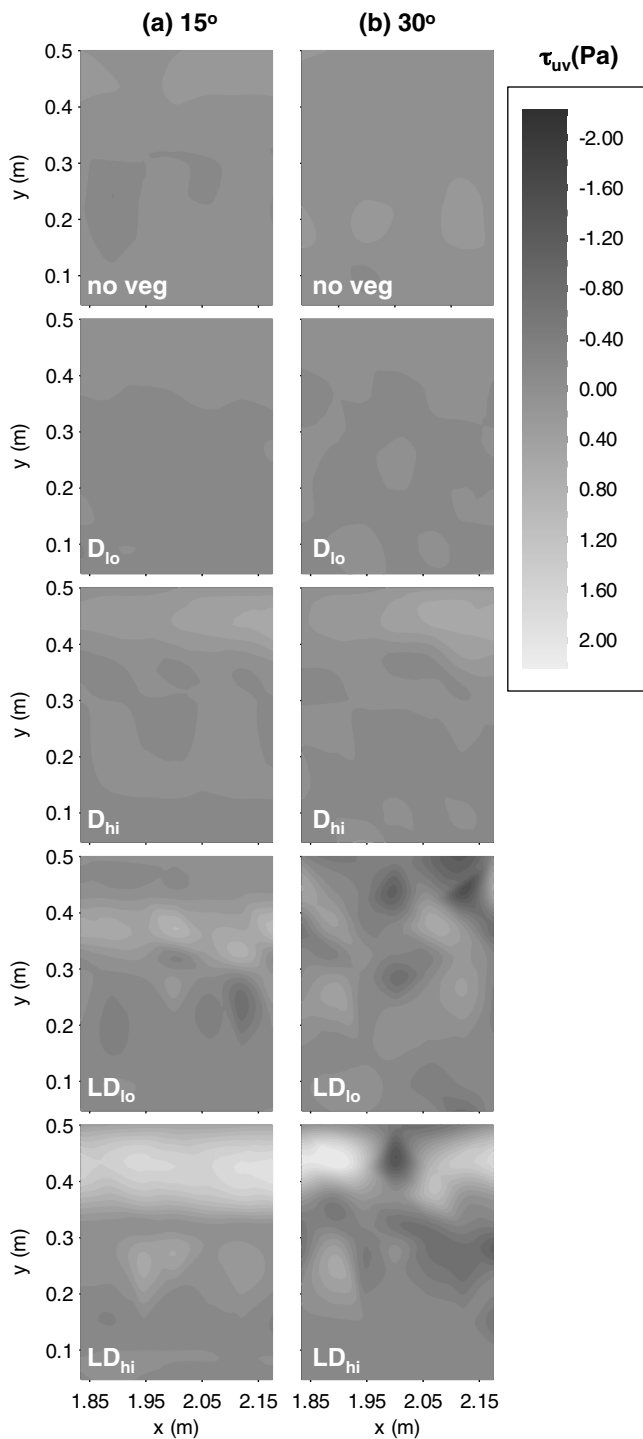


Fig. 3. Spatial patterns of vertical Reynolds stress (τ_{uv} , Pa) for the (a) 15° and (b) 30° bank surfaces; D_{lo} , D_{hi} , LD_{lo} , and LD_{hi} are defined in Fig. 1; the solid line represents the base of the bank slope

was present, but neither τ_{uv} nor τ_{uw} was consistently dominant when vegetation was present.

Summary and Conclusions

This paper has presented results from an experimental study aimed at characterizing the influence of bank angle and vegetation density on near-bank patterns of shear stress and turbulence. The key findings of the study are:

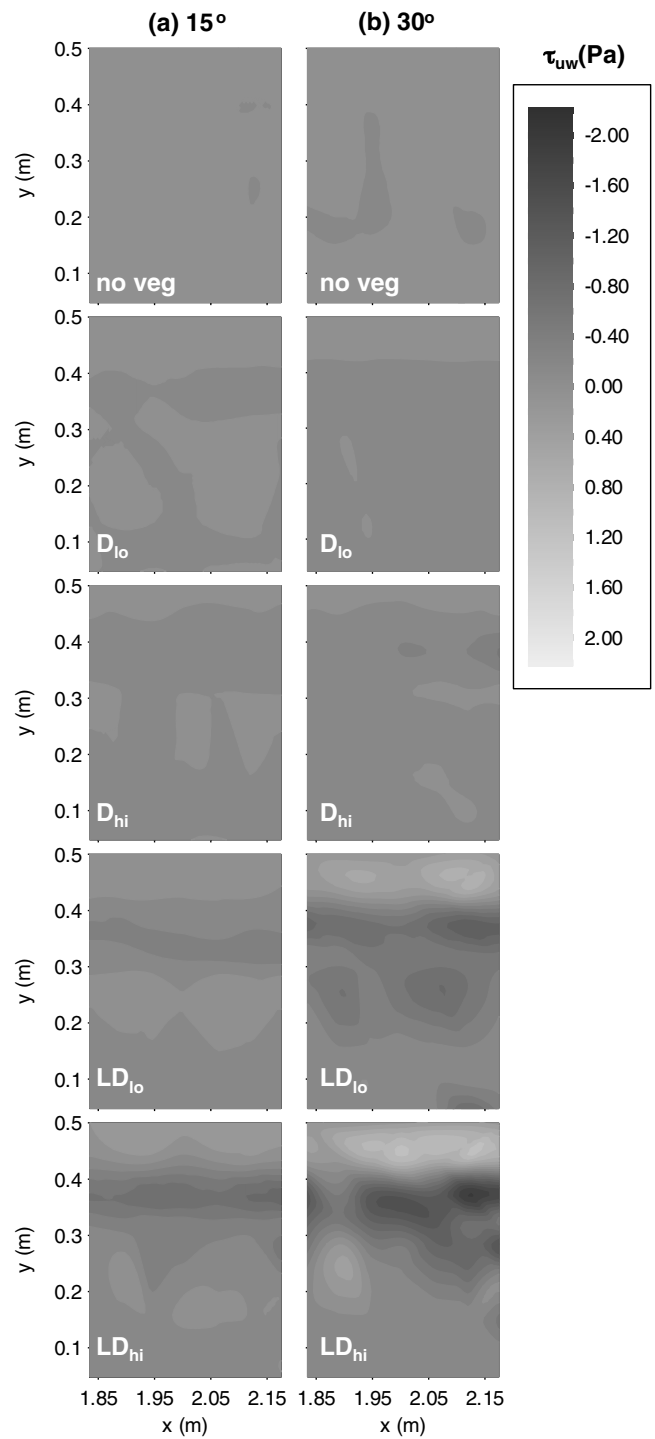


Fig. 4. Spatial patterns of lateral Reynolds stress (τ_{uw} , Pa) for the (a) 15° and (b) 30° bank surfaces; D_{lo} , D_{hi} , LD_{lo} , and LD_{hi} are defined in Fig. 1; the solid line represents the base of the bank slope

1. Increasing bank angle caused increased turbulence intensities and Reynolds stresses at the base of the bank slope. However, on the bank slope itself, relative turbulence intensities and Reynolds stresses were insensitive to the angle of the bank.
2. Increasing vegetation density on the bank surface caused increased near-bed turbulence intensities and Reynolds stresses in the main channel and at the base of the slope. These increases were particularly evident along the base of the slope, supporting the findings of previous studies (e.g., Yang et al. 2007; Gorrick 2009; Hopkinson and Wynn 2009).

3. Relative turbulence intensities and Reynolds stresses were higher for leaved than for leafless conditions. This result highlights the importance of including leaves or equivalent canopy roughness in both flume and numerical experiments and casts doubt on the results of studies that have not done so. The additional frontal area afforded by a canopy and the hydraulic behavior of a canopy cannot be replicated by merely increasing stem density but instead require the use of vegetative elements of a more realistic morphology (e.g., Yang et al. 2007; Hopkinson and Wynn 2009).

It is acknowledged that the strength of these conclusions may be reduced by the lack of uniform flow in the flume and the authors, therefore, encourage future studies to more carefully develop uniform flow conditions (Tracy and Lester 1961). Nonetheless, the results presented in this paper contribute to the growing knowledge (e.g., Nepf 1999; Wilson et al. 2003; McBride et al. 2007; Yang et al. 2007; Gorrick 2009; Hopkinson and Wynn 2009) of the influence of vegetation morphology and configuration on near-boundary hydraulics. Furthermore, they emphasize the need to consider the morphology of vegetation when assessing turbulence and stress within patches of vegetation and to evaluate the importance of the timing of flood events relative to leaf-out when planting vegetation as a management strategy to deflect near-bank flows.

Acknowledgments

Support for this research was provided by an NSF IGERT graduate fellowship (NSF award 0333257) in the Ecosystem Informatics IGERT program at Oregon State University and the USDA-ARS National Sedimentation Laboratory at Oxford, Mississippi. Cross-sections at the Goodwin Creek bendway site were surveyed by staff of the Watershed Physical Processes Research Unit of the USDA-ARS-NSL. The authors appreciate advice provided by Vincent Neary. The authors are also grateful for technical advice and review provided by Daniel Wren and technical assistance provided by Lee Patterson. This manuscript was greatly improved by the comments of four anonymous reviewers, the associate editor, and the editor.

References

- Biron, P. M., Robson, C., Lapointe, M. F., and Gaskin, S. J. (2004). "Comparing different methods of bed shear stress estimates in simple and complex flow fields." *Earth Surf. Processes Landforms*, 29(11), 1403–1415.
- Czarnomski, N. M. (2010). "Influence of vegetation on streambank hydraulics." Ph.D. thesis, Oregon State Univ., Corvallis, OR.
- Freeman, G. E., Rahmeyer, W. H., and Copeland, R. R. (2000). "Determination of resistance due to shrubs and woody vegetation." *ERDC/CHL Technical Report 00-25*, U.S. Army Corps of Engineers, Vicksburg, MS.
- Goring, G., and Nikora, V. (2002). "Despiking acoustic doppler velocimeter data." *J. Hydraul. Eng.*, 128(1), 117–126.
- Gorrick, S. (2009). "Field and laboratory investigations on the effects of riparian vegetation on stream flow and sediment dynamics." *Proc., 33rd IAHR Congress (CD-ROM)*, IAHR, Madrid, Spain.
- Hinze, J. O. (1975). *Turbulence*, 2nd Ed., McGraw Hill, NY.
- Hopkinson, L., and Wynn, T. (2009). "Vegetation impacts on near bank flow." *Ecohydrol.*, 2(4), 404–418.
- Julien, P. Y. (2002). *River mechanics*, Cambridge University Press, New York.
- Langendoen, E. J., and Simon, A. (2008). "Modeling the evolution of incised streams. II: Streambank erosion." *J. Hydraul. Eng.*, 134(7), 905–915.
- McBride, M., Hession, W. C., Rizzo, D. M., and Thompson, D. M. (2007). "The influence of riparian vegetation on near-bank turbulence: A flume experiment." *Earth Surf. Processes Landforms*, 32(13), 2019–2037.
- Nepf, H. M. (1999). "Drag, turbulence, and diffusion in flow through emergent vegetation." *Water Resour. Res.*, 35(2), 479–489.
- Niklas, K. J. (1992). *Plant biomechanics*, Univ. of Chicago Press, Chicago.
- Robert, A. (2003). *River processes: An introduction to fluvial dynamics*, Oxford University Press, New York.
- Schlichting, H. (1968). *Boundary layer theory*, McGraw-Hill, New York.
- Simon, A., and Collison, A. J. C. (2002). "Quantifying the mechanical and hydrologic effects of riparian vegetation on streambank stability." *Earth Surf. Processes Landforms*, 27(5), 527–546.
- Simon, A., Curini, A., Darby, S. E., and Langendoen, E. J. (2000). "Bank and near-bank processes in an incised channel." *Geomorphol.*, 35(3–4), 193–217.
- Sukhodolov, A. N., and Rhoads, B. L. (2001). "Field investigation of three-dimensional flow structure at stream confluences: 2. Turbulence." *Water Resour. Res.*, 37(9), 2411–2424.
- Tracy, H. J., and Lester, C. M. (1961). "Resistance coefficients and velocity distribution, smooth rectangular channel." *Geological Survey Water-Supply Paper, 1592-A*. U.S. Government Printing Office, Washington, DC.
- Wahl, T. (2009). "WinADV version 2.027." U.S. Bureau of Reclamation, Water Resources Research Laboratory, Denver, CO.
- White, B. L., and Nepf, H. M. (2008). "A vortex-based model of velocity and shear stress in a partially vegetated shallow channel." *Water Resour. Res.*, 44(1), W01412–W01426.
- Wilkerson, G. V. (2007). "Flow through trapezoidal and rectangular channels with rigid cylinders." *J. Hydraul. Eng.*, 133(5), 521–533.
- Wilson, C. A. M. E., Stoesser, T., Bates, P. D., and Batemann Pinzen, A. (2003). "Open channel flow through different forms of submerged flexible vegetation." *J. Hydraul. Eng.*, 129(11), 847–853.
- Wilson, C. A. M. E., Yagci, O., Rauch, H.-P., and Stoesser, T. (2006a). "Application of the drag force approach to model the flow-interaction of natural vegetation." *Int. J. River Basin Manage.*, 4(2), 137–146.
- Wilson, C. A. M. E., Yagci, O., Rauch, H.-P., and Olsen, N. R. B. (2006b). "3D numerical modelling of a willow vegetated river/floodplain system." *J. Hydrol.*, 327(1–2), 13–21.
- Wood, A. L., Simon, A., Downs, P. W., and Thorne, C. R. (2001). "Bank-toe processes in incised channels: The role of apparent cohesion in the entrainment of failed bank materials." *Hydrol. Processes*, 15(1), 39–61.
- Yalin, M. S. (1971). *Theory of hydraulic models*, Macmillan, London.
- Yang, K., Cao, S., and Knight, D. W. (2007). "Flow patterns in compound channels with vegetated floodplains." *J. Hydraul. Eng.*, 133(2), 148–159.
- Zong, L., and Nepf, H. M. (2010). "Flow and deposition in and around a finite patch of vegetation." *Geomorphol.*, 116(3–4), 363–372.